Ministry of Higher Education

and Scientific Research

Journal of Kufa for Chemical Sciences

A refereed

Research Journal Chemical Sciences

Vol.2 No.9 Year 2022

ISSN 2077-2351

Upgrading API and Specific Gravity Specifications of Iraqi Crude Oil Using a Laboratory-Built Multipumping Fuel Analysis (MPFA) System

Ahmed Abdulrazzaq Hadi,

Mohammed Turki khathi and Ali Abdulkhabeer Ali

[1]Department of Chemistry, College of Science, University of Thi-Qar, Thi-Qar, Iraq.

Corresponding author: ahm.abd.ch@sci.utq.edu.iq

Abstract

Iraqi heavy crude oil (26.85 API) is processed by a laboratory-made fuel injection system and through the deasphalting oil (DAO) extraction process by different solvents and the application of different variables. The system was built with low-cost parts found in local markets. The purpose of a manufactured fuel system is to enhance the API and specific gravity (Sp.gr.) specifications of the collected samples and obtain the reduced crude oil through the DAO process. The extraction was carried out with a temperature range, a solvent flow rate, a mixing coil length, a solvent entry time, and different types of solvents. In general, results show that the API and Sp.gr of DAO increased from 26.85 and 0.8936 to 39.28 and 0.8132, respectively. Also, sulfur content decreased from 4.1967 wt.% to 2.201 wt.% at optimum conditions. The semi-automated MPFA system was successfully used to enhance crude oil specifications sensitive and accurate manner.

Keywords: MPFA system, crude oil, variables, upgrading specifications.

1. Introduction

The API and specific gravity of crude oil are two parameters that have found major applications in the industry for determining the character and quality of crude oil [1,2]. Specific gravity and API ratios are used to assess crude oil quality during production and to determine its trade price. Lighter (high API) crudes are generally more desirable because they yield more high-value light products when processed [3,4]. Crude oils differ significantly in terms of the chain lengths of constituent hydrocarbons and other components (such as sulfur) depending on their origin and are thus classified into three categories: light, medium, and heavy [5]. Light oil is often in the 35–45 API range, which contains the majority of the highest-valued crudes such as Brent and WTI. Crudes lighter than 45 API degrees are classified as "extra-light crude" or condensates and are valued more than light crude because they contain a high concentration of light ends such as propane and butane.

Medium crude has an API of 25–35, while heavy crude has an API of 15–25. Anything less than 15 API is termed "extra-heavy crude" [6]. Temperature has an effect on API. API gravity rises when temperatures rise, although specific gravity falls as temperatures rise. The standard measuring temperature for the API and specific gravity by density meter is 15 °C or 60 °F [7–11]. The main goal of this work is to build a semi-automated MPFA system and use it to improve the API and specific gravity of crude oil from Iraq, which is a major economic resource.

2. Experimental

2.1 Crude oil feedstock

The actual crude oil sample that was used in this experiment was examined in the lab of the Nasiriyah Oil company. The crude oil used was heavy crude oil due to its 0.8936 specific gravity and 26.85 API according to ASTM D-3297, a high sulfur content of 4.1967 wt.% based on ASTM D-4294, and asphalt content of 2.4873 wt.%.

2.2 Materials

During an analytical application with a multipumping fuel analysis system, high-purity solvents were used in the fuel injection system. The chemical materials used in the study are listed in Table 1.

Table 1. Chemicals employed in the MPFA system

No.	Name	Chemical Formula	Molecular weight	Purity%	Supplier
1	n- Heptane	C_7H_{16}	100.21	99 %	CDH
2	n- Hexane	C_6H_{14}	86.18	99.5 %	CDH
3	Acetone	C_3H_6O	58.08	99.5 %	CDH
4	Acetonitrile	CH_3CN	41.05	99 %	CDH
5	Ethanol	C_2H_5OH	46.07	99.7 %	CDH

2.3 Lab-Built Semi-Automated MPFA system

The fuel injection system that was constructed in the laboratory is depicted in Fig. 1, and Table 2 provides information on each of the system's individual components.

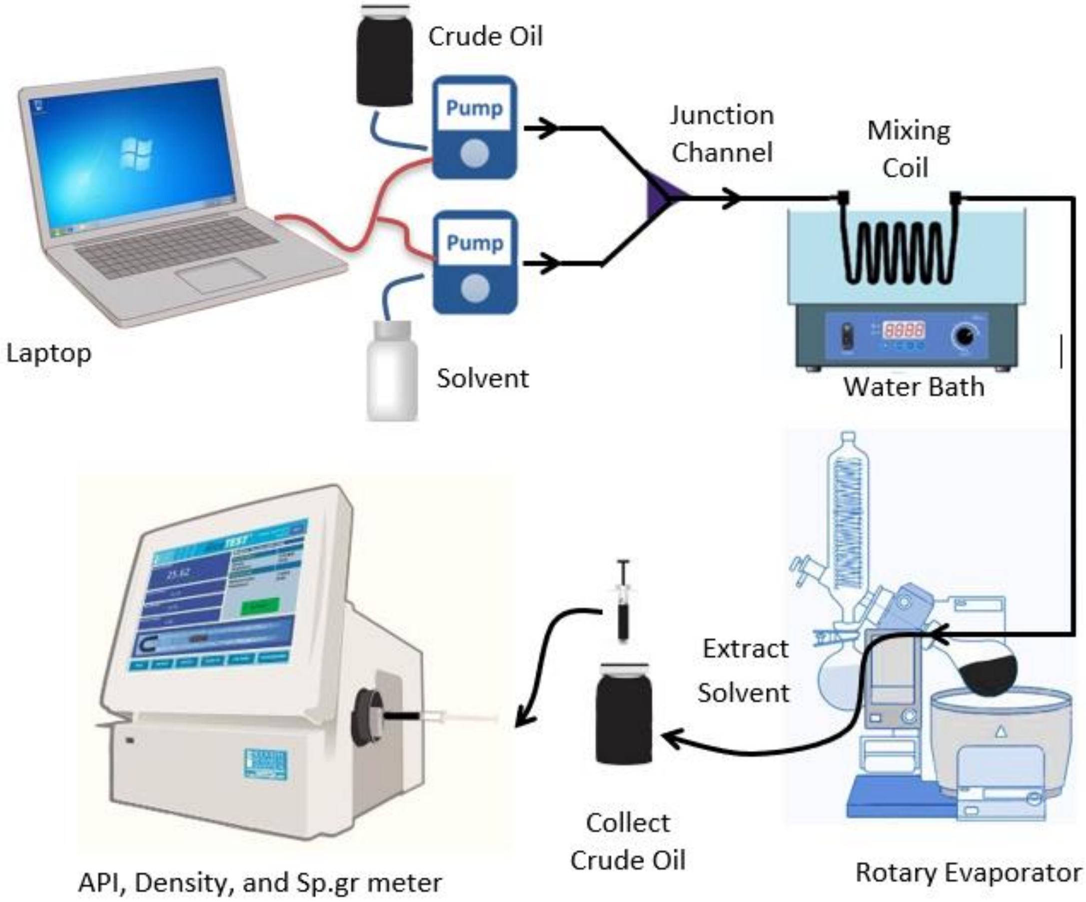

Fig. 1: Diagram of Semi-Automated MPFA-density meter System

Table 2. Components MPFA system

Component	Work	Origin
Peristaltic Pump	Pulling liquids	China
Arduino Uno	Microcontroller	China
Driver Motor L298N	Microcontroller	China
Power Supply	DC Electrical source	China
Mixing Coil	Mixing liquids	Lab-made
Water bath	Heating of Mixture	Korea
Rotary Evaporator	Solvent Extraction	Korea
Density meter	measure density, specific gravity, and API	United States of America

2.4 Design of experiment

To minimize the number of tests, the experimental parameters were optimized using a central composite design (CCD) as part of an investigation into the performance of the semi-automated system [12]. To carry out the experimental design, data analysis, model fitting, and graph plotting, Design Expert version 13 software was used [13]. Table 4 shows the details of the central composite design and the API and specific gravity results for each experiment.

2.5 Procedure

The MPFA system is constructed according to Fig. 1. The system is operated using special software that controls the time of turning on and off the system and the speed of rotation of the pumps that withdraw the crude oil and solvents. The crude oil and solvents are drawn into the mixing coil. The copper mixing coil is placed in a water bath for heating at different temperatures. After the mixture comes out of the coil and into the rotary evaporator, the crude oil is extracted and taken to the density analyzer. The digital density analyzer (DM 2911) is in compliance with the test method (ASTM D5002), and the test procedure allows for the determination of crude oil's density, specific gravity, and API. Add 1 to 2 mL of crude oil using a suitable syringe to the instrument's sample tube, which needs to be clean and dry. Before evaluating the test sample, let the sample equilibrate to the test temperature. After the instrument consistently produces a reading of four significant figures for each density, specific gravity, and API gravity measurement, note the findings [14]. During our work, five variables from five levels are applied to show their impact on the specification improvement process. These variables and their levels are listed in Table 3.

Table 3: variables utilized in the MPFA system

Parameter	Symbol	Values				
		Level 1	Level 2	Level 3	Level 4	Level 5
Solvent Type	A	n-Heptane	n-Hexane	Acetone	Acetonitrile	Ethanol
Flow Rate mL/min	B	10	17.5	25	32.5	40
Coil Length cm	C	120	140	160	180	200
Temperature ^{o}C	D	30	37.5	45	52.5	60
Delay time sec	E	0	15	30	45	60

3. Results and Discussion

3.1 Design and response

The design shown by CCD in Table 4 contains many variables (solvent type, solvent flow rate, mixing coil length, temperature, and time) with API and specific gravity responses. Several factors were examined at to figure out how to get high sensitivity and good use of the solvent.

Table 4. CCD design of the experiments and investigated response

Run no.	Operating parameters					API	Sp.gr
	Solvent type	Flowrate mL/min	Coil length cm	Temp. ^{o}C	Time Sec		
1	n-Hexane	17.5	180	37.5	15	34.75	0.8511
2	n-Hexane	17.5	140	52.5	15	32.78	0.8613
3	n-Hexane	32.5	140	52.5	45	34.89	0.8504
4	n-Hexane	17.5	140	37.5	15	29.57	0.8788
5	n-Hexane	17.5	180	37.5	45	31.29	0.8692
6	n-Hexane	17.5	180	52.5	45	31.36	0.8688
7	n-Hexane	32.5	140	52.5	15	34.49	0.8524
8	n-Hexane	17.5	140	37.5	45	30.9	0.8713
9	n-Hexane	17.5	140	52.5	45	31.36	0.8688
10	n-Hexane	17.5	180	52.5	15	33.32	0.8585
11	n-Hexane	32.5	140	37.5	45	32.45	0.863
12	n-Hexane	32.5	180	52.5	45	33.61	0.857
13	n-Hexane	32.5	140	37.5	15	33.92	0.8553
14	n-Hexane	32.5	180	52.5	15	35.49	0.8473
15	n-Hexane	32.5	180	37.5	15	35.17	0.8489
16	n-Hexane	32.5	180	37.5	45	34.57	0.852
17	Acetone	25	160	45	30	33.39	0.8581
18	Acetone	25	160	60	30	34.49	0.8524
19	Acetone	40	160	45	30	36.71	0.8412
20	Acetone	25	160	30	30	35.27	0.8484
21	Acetone	25	120	45	30	34.94	0.8501
22	Acetone	25	160	45	60	34.33	0.8532
23	Acetone	10	160	45	30	34.03	0.8548
24	Acetone	25	200	45	30	37.62	0.8366
25	Acetone	25	160	45	0	36.19	0.8285
26	n-Heptane	25	160	45	30	39.28	0.8132
27	Ethanol	25	160	45	30	39.01	0.8298
28	Acetonitrile	32.5	140	52.5	45	34.26	0.8536
29	Acetonitrile	17.5	160	37.5	45	34.33	0.8532

30	Acetonitrile	32.5	160	52.5	45	36.97	0.8399
31	Acetonitrile	32.5	140	37.5	45	33.74	0.8563
32	Acetonitrile	32.5	140	37.5	15	35.12	0.8492
33	Acetonitrile	32.5	140	52.5	15	35.66	0.8464
34	Acetonitrile	17.5	140	37.5	15	31.46	0.8683
35	Acetonitrile	32.5	160	37.5	45	34.99	0.8499
36	Acetonitrile	32.5	160	37.5	15	35.86	0.8454
37	Acetonitrile	32.5	160	52.5	15	35.29	0.8483
38	Acetonitrile	17.5	160	37.5	15	33.57	0.8572
39	Acetonitrile	17.5	140	52.5	45	31.29	0.8692
40	Acetonitrile	17.5	140	52.5	15	33.25	0.8588
41	Acetonitrile	17.5	160	52.5	15	34.26	0.8536
42	Acetonitrile	17.5	140	37.5	45	31.36	0.8688
43	Acetonitrile	17.5	180	52.5	45	35.47	0.8474

3.2 Process Graph Interpretation

The normal distribution of the data (shown in Fig. 2) makes it evident that the difference between the actual value and the expected value in data analysis is a crucial aspect of model interpretation. If the actual results and the predicted results are close to the line in italics [15], the results are more accurate.

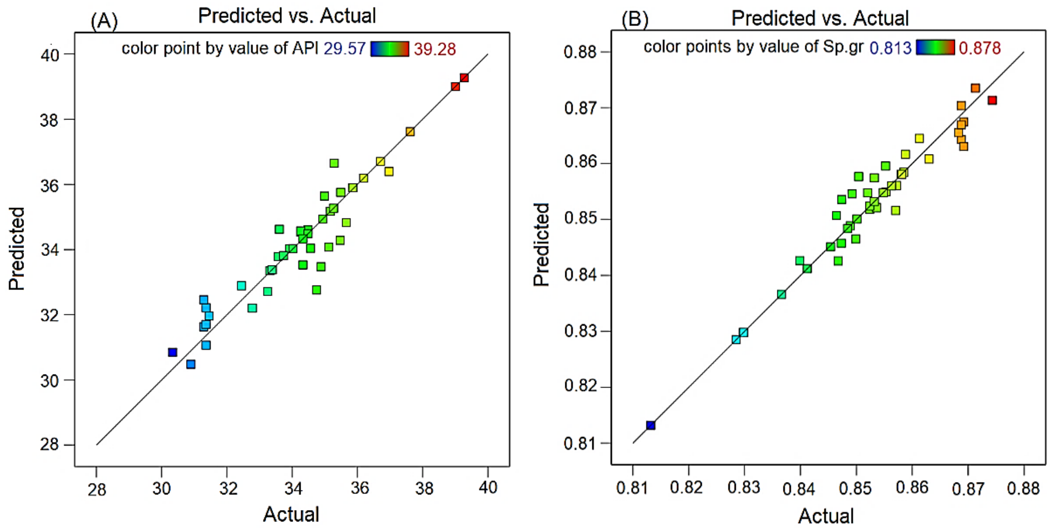

Fig. 2: Actual vs. predicted value of the A: API and B: Sp.gr

3.3 Analysis of variance

The statistical significance of model components and their interactions were evaluated using the analysis of variance (ANOVA) [16]. The model coefficients for the process were evaluated for significance based on their respective F and p-values at a 0.05 level of confidence [17]. Based on Table 5, the ANOVA table results demonstrated the strong significance of the quadratic models [18], which is supported by a p-value of less than 0.05 and the large model F-values of 45.93 and 69.29 for API and specific gravity, respectively. Additionally, the coefficient of variation (CV) has values of 2.37 and 0.499 % for API and specific gravity, respectively. According to the values of the CV indices, the models are very reliable and accurate in the experiments and are repeatable; the model that has a CV value under 10% is regarded as having sufficient repeatability [19].

Table 5. ANOVA results for API and Specific gravity models

Response	Source	Term df	Error df	F-value	p- value	
API	**Whole plot**	4	26.00	45.93	< 0.0001	significant
	a-A	4	26.00	45.93	< 0.0001	
	Subplot	22	26.00	6.31	< 0.0001	significant
	B-B	1	26.00	27.00	< 0.0001	
	C-C	1	26.00	20.15	0.0001	
	D-D	1	26.00	3.43	0.0756	
	E-E	1	26.00	0.4012	0.5320	
	BC	1	26.00	3.79	0.0623	
	BD	1	26.00	0.0492	0.8262	
	BE	1	26.00	0.0003	0.9863	
	CD	1	26.00	3.19	0.0856	
	CE	1	26.00	0.0366	0.8498	
	DE	1	26.00	0.0100	0.9211	
	B^2	1	26.00	9.70	0.0044	
	C^2	1	26.00	20.67	0.0001	
	D^2	1	26.00	5.50	0.0270	
	E^2	1	26.00	8.66	0.0068	
Sp.gr	**Whole plot**	4	26.00	69.29	< 0.0001	significant
	a-A	4	26.00	69.29	< 0.0001	
	Subplot	22	26.00	7.12	< 0.0001	significant
	B-B	1	26.00	26.34	< 0.0001	
	C-C	1	26.00	19.72	0.0001	
	D-D	1	26.00	3.33	0.0796	
	E-E	1	26.00	0.4239	0.5207	
	BC	1	26.00	4.03	0.0552	
	BD	1	26.00	0.0795	0.7801	
	BE	1	26.00	0.0001	0.9934	
	CD	1	26.00	3.33	0.0795	
	CE	1	26.00	0.0248	0.8760	
	DE	1	26.00	0.0017	0.9672	

B^2	1	26.00	9.19	0.0055
C^2	1	26.00	19.60	0.0002
D^2	1	26.00	5.34	0.0290
E^2	1	26.00	26.80	< 0.0001

3.4 Interpreting the coefficient of determination

The ability of a statistical model to predict an outcome is measured by the coefficient of determination (R^2) [20]. The R^2 and adjusted R^2 values shown in Table 6 were extremely near 1, and the response quadratic model equations showed a reasonable agreement with a difference between the two of less than 0.2. Therefore, the validity of the experimental data and the predictability of the models are thus demonstrated by these outcomes.

Table 6. The goodness of fit of a statistical model for API and Sp.gr

Response	R^2	Adjusted R^2	Std. Dev	Mean	C.V %
API	0.9273	0.8424	0.8131	34.29	2.37
Sp.gr	0.9458	0.8826	0.0043	0.8527	0.4998

In the case of the n-heptane solvent, the empirical relationships between the factor variables and the responses are shown by formulas 1 and 2.

API=73.67416 + 0.02433 B - 0.41139 C - 0.26149 D - 0.15422 E -0.00186 B * C - 0.00056 B * D + 2.22222 e-05 B * E - 0.00171 C * D 9.16666 e-05 C * E + 0.00012 D * E + 0.0088 B^2 + 0.00180 C^2 + 0.00662 D^2 + 0.00207 E^2. ……………………………………………………(1).

Sp.gr = 0.63721 - 0.00026 B + 0.00206 C + 0.00126 D + 0.00127 E + 1.00833e-05 B * C + 3.777776e-06 B * D - 5.55555 e-08 B * E + 9.16666 e-06 C * D - 3.958333e-07 C * E - 2.77777 e-07 D * E - 4.48888 e-05 B^2 - 9.21875 e-06 C^2 - 3.42222 e-05 D^2 -1.916666 e-05 E^2…………………………………………………………………(2)

B = flow rate; C = mixing coil length; D = temperature, and E = time, while two variables indicate an interaction effect.

3.5 One Factor Effect

3.5.1 Effect of solvent type

The solubility of asphaltene decreases in the medium with polar solvents such as ethanol and acetonitrile, and the solubility factor increases when using non-polar solvents such as n-hexane, and n-heptane [21]. Asphaltene is less soluble in polar solvents like ethanol and acetonitrile, while non-polar solvents like n-hexane and n-heptane have a higher solubility factor [22]. The impact of different utilized solvents on the asphaltene content percentage is shown in Fig. 3 (A and F) for API and Sp.gr., respectively. The results were attributed to the breakdown of the asphalt aggregate and a decrease in micelle-like clusters, which aided in the deasphalting process. Additionally, the solvent scattered asphaltene molecules, resulting in a decrease in both the amount of asphaltene and the size of the asphaltene molecule [23]. When comparing the results to those obtained when n-heptane was used as the solvent, it was found that lowering the solvent's carbon number decreased the DAO yield, which in turn decreased the pitch or precipitated fraction yield [24–29]. This is due to the solvent's ability to solubilize heavier hydrocarbons when its molecular weight is increased [25,28]. This is demonstrated by the solubility parameter of asphaltic compounds in various solvents [28]. This can also be attributed to the resins and their impact on the deasphalting process, as well as the fact that they precipitated in greater proportion when the solvent had a larger molecular weight [30]. It was found that the use of an n-heptane solvent had the best effect on the process of removing asphalt, as it reduced the density to 0.8107 g/cm3, the specific gravity to 0.8132, the sulfur content to 2.201 wt.%, and the kinematic viscosity to 1.037 cSt, while increasing the API value to 39.28 in the presence of interaction with other influences when compared to the untreated crude oil sample. From Fig. 4-E, a higher reduction in asphaltene content is obtained with an n-heptane solvent. The best asphaltene extraction efficiency was at a 3/4:1 ratio of n-heptane to crude oil.

3.5.2 Effect of flow rate

The impact on the deasphalting process is seen in Fig. 4 (B and G) for API and Sp.gr., respectively, at various flow rates. The deasphalting process for heavy crude oil was enhanced by increasing flow rates from 10 to 40 mL/min. Fig. 3 (B and G) shows the extraction of asphaltene that was studied using a different solvent-to-oil ratio (SOR), since the crude oil flow rate was constant at 40 mL/min while the solvent flow rates were from 10 to 40 mL/min. The best value for flow rate according to a design expert's software was 31 mL/min of the n-heptane solvent according to Fig. 5, which is approximately a ratio of 3/4:1 SOR. The breakdown of asphalt agglomerates and the lowering of micelle-like clusters were critical in improving crude oil characterizations, where such solvents dispersed asphaltene molecules to reduce their molecular size and decreased the number of asphaltic compounds, resulting in an improvement in other crude oil characterizations such as API and Sp.gr asphaltene content and sulfur content [31]. Since the p-value is less than 0.05, the ANOVA table shows that the solvent flow rate has a significant effect on the deasphalting process.

3.5.3 Effect of Mixing coil length

The effect of mixing coil lengths was studied, as shown in Fig. 3 (C and H) for API and Sp.gr., respectively. This process in general increases the amount of asphalt extraction using n-heptane solvent. Experimental evidence suggests that asphaltene precipitation is a dynamic process involving the aggregation and reorganization of aggregates [32]. The deasphalting efficiency increases as the mixing coil's length increases from 120 to 200 cm because a longer coil length allows for a high mixing efficiency between the crude oil and the solvent, which allows the solvent to extract asphaltic compounds more effectively. Another possible reason that may affect the mixing coil is its geometry. The mixing coil is wrapped in a helical shape; this allows the solvents to disperse in the crude oil in both axial and radial ways, which in turn led to an increase in the efficiency of the mixing and extraction processes [33]. As shown in Table 5, the mixing coil length variable has a significant effect on the deasphalting process since the p-value is less than 0.05.

3.5.4 Effect of Temperature

Fig. 3(D and I) of API and Sp.gr demonstrates that the deasphalting process decreases as temperature rises (from 30 to 60 oC). Similar results have been reported in previous investigations [34]. By increasing the extraction temperature, the amount of asphaltene removed is decreased. This is because the solvent's density dropped by raising the extraction temperature, which decreased the solvent's ability to dissolve heavier molecules [35]. This resulted in an improvement in the quality of the deasphalted residue at the cost of a lower yield of the deasphalted residue and reducing the yield of the deasphalted waste while enhancing the quality of the deasphalted residue, resulting in a wider region of immiscibility in a system with solvent and crude oil. Another possible reason for decreasing asphalt removal effectiveness is the increased solubility of heavier and resinous components of reduced crude with rising extraction temperatures, which allows asphaltenes and resin components to escape to the oil phase. The pitch precipitation reduced as the temperature increased, consistent with previous observations [36]. Hence, 32 oC is a suitable extraction temperature, at which asphaltene removal was about 57.94 wt%.

3.5.5 Effect of Time

The delay time of the solvent used in our work is the time when the solvent enters the system after the crude oil enters it. The results of the experiments show that the extraction of asphaltene from crude oil is most effective when there is little time between the entry of the solvent and the crude oil into the system. This can be explained by lengthening the time and amount of the solvent mixing process with the crude oil [37], which in turn improves the extraction process efficiency, as shown in Fig. 3 (E andJ).

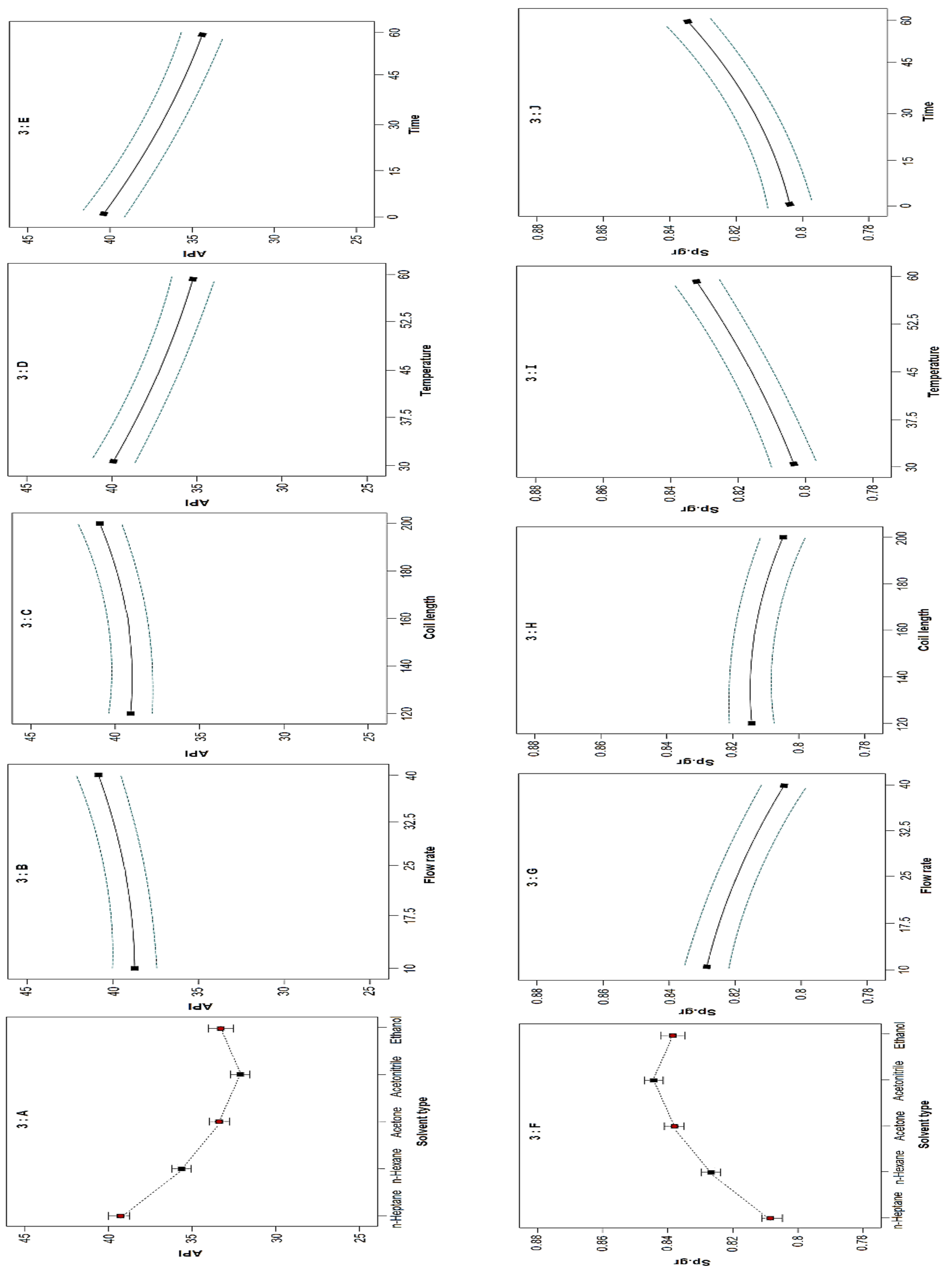
3 : A
3 : B
3 : C
3 : D
3 : E
3 : F
3 : G
3 : H
3 : I
3 : J
API
Sp.gr
n-Heptane
n-Hexane
Acetone
Acetonitrile
Ethanol
Solvent type
Flow rate
Coil length
Temperature
Time

Fig. 3:(A to E) One factor effect on API; and 3:(F to J) One factor effect on Sp.gr.

3.6 Response parameter optimization

Derringer's desirability function was used in the Design-Expert software to implement the numerical optimization study of the process parameters. A statistical design method known as a desirability function measures the ideal input parameter values in order to select the best performance levels for one or more output variables or responses [38]. The scale of desirability ranges from 0 to 1, with a value of 0 signifying fully undesired for the variable under consideration and a value of 1 signifying completely desirable [39]. For each input variable and response, numerical optimization enables the selection of a desirable value in the form of a range, goal, minimum, or maximum value. Five parameters were analyzed in our investigation to determine the values that have the highest API and lowest Sp.gr as a result of the fuel injection system. For maximum desirability, flow rate, mixing coil length, temperature, and delay time were set in the range of 10–40 mL/min, 120–200 cm, 30–60 oC, and 0–60 sec, respectively. obtained optimum operating conditions, as shown in Fig. 4, in which 31 mL/min of flow rate, 172 cm of mixing coil length, 34 oC of temperature, and 5 sec of time were the best conditions for n-heptane solvent.

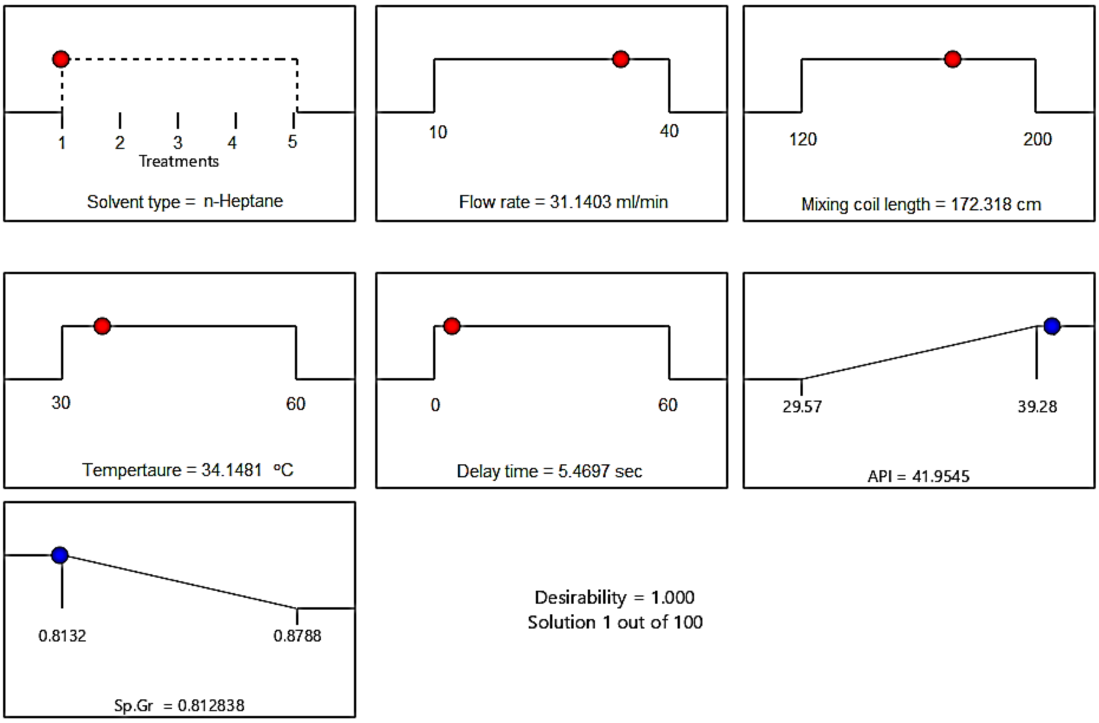

Fig 4. Scheme of the process desirability

It was determined that the impact on API gravity of using variables occurs in the following order: mixing coil length > time > temperature > solvent flow rate in n-heptane solvent. whereas the following order had an impact on the specific gravity:

mixing coil length > temperature > time > solvent flow rate for n-heptane solvent according to formulas 1 and 2, respectively. These operating factors yield theoretical and practical API values of 41.95 and 39.28 and Sp.gr values of 0.8132 and 0.8128, respectively. These values are considered economically and practically beneficial when compared with other studies.

4. Conclusion

According to the results obtained, the fuel system we designed and implemented is one consider to be highly effective. as the system's accuracy was high due to the precise electronic control, where computer software was used to control the volume withdrawal in milliliters of high-viscosity crude oil. This method is appropriate for assuring the stability of liquid mixing times and the ability to operate with a larger range of effects. It is also a cost-effective approach for recovering the used solvent. It does, however, decrease the operator's exposure to chemical risks. All these features distinguish the method of fuel injection system designed in this study, as it proved its efficiency in enhancing the API and Sp.gr. of the crude oil from 26.85 and 0.8936 to 39.28 and 0.8132, respectively.

References

1. Demirbas, A., Alidrisi, H., & Balubaid, M. A. [2015]: API gravity, sulfur content, and desulfurization of crude oil. Petroleum Science and Technology, 33(1), p.93-101.
2. Villasana, Y., Ramírez, S., Ancheyta, J., & Brito, J. L. [2014]: Effect of hydrotreating reaction conditions on viscosity, API gravity and specific gravity of Maya Crude Oil. In Computational and Experimental Fluid Mechanics with Applications to Physics, Engineering and the Environment (p.423-430). Springer, Cham.
3. Ghulam, Y., Muhammad, I. B., Tariq, M. A., Syed, M. S. R. N., Muhammad, A., Khizar, A., & Farah, N. T. [2013]: Quality and chemistry of crude oils. Journal of Petroleum Technology and Alternative Fuels, 4(3), p.53-63.
4. Brown, P., Fergusson, I. F., Pirog, R. L., Ramseur, J. L., Ratner, M., & Vann, A. [2014]. US crude oil export policy: Background and considerations. Congressional Research Service.
5. Doust, A. M., Rahimi, M., & Feyzi, M. [2015]: Effects of solvent addition and ultrasound waves on viscosity reduction of residue fuel oil. Chemical engineering and processing: Process intensification, 95, p. 353-361.
6. Pasquini, C., & Bueno, A. F. (2007). Characterization of petroleum using near-infrared spectroscopy: Quantitative modeling for the true boiling point curve and specific gravity. Fuel, 86(12-13), p.1927-1934.
7. Onojake, M. C., Osuji, L. C., & Oforka, N. C. [2013]: Preliminary hydrocarbon analysis of crude oils from Umutu/Bomu fields, southwest Niger Delta Nigeria. Egyptian Journal of Petroleum, 22(2), p.217-224.
8. Appenteng, M. K., Golow, A. A., Carboo, D., Narley, V. K., Kaka, E. A., Salifu, M., & Aidoo, F. [2013]: Physicochemical characterization of the Jubilee crude oil. Appl Chemistry, 54, p. 12513-12517.

9. Demirbas, A., & Al-Ghamdi, K. [2015]. Relationships between specific gravities and higher heating values of petroleum components. Petroleum science and technology, 33(6), p.732-740.
10. Dickson, U. J., & Udoessien, E. I. [2012]: Physicochemical studies of nigeria's crude oil blends. Petroleum & Coal, 54(3).
11. Sad, C. M., da Silva, M., dos Santos, F. D., Pereira, L. B., Corona, R. R., Silva, S. R., & Lacerda Jr, V. [2019]: Multivariate data analysis applied in the evaluation of crude oil blends. Fuel, 239, p.421-428.
12. Mazaheri, H., Ghaedi, M., Asfaram, A., & Hajati, S. [2016]: Performance of CuS nanoparticle loaded on activated carbon in the adsorption of methylene blue and bromophenol blue dyes in binary aqueous solutions: using ultrasound power and optimization by central composite design. Journal of Molecular Liquids, 219, p. 667-676.
13. Kumar, S., Ali, J., & Baboota, S. [2016]: Design Expert® supported optimization and predictive analysis of selegiline nanoemulsion via the olfactory region with enhanced behavioural performance in Parkinson’s disease. Nanotechnology, 27(43), p. 435101.
14. Cani, X., Malollari, I., Beqiraj, I., Manaj, H., Premti, D., & Lorina, L. İ. Ç. İ. [2016]: Characterization of crude oil from various oilfields in Albania through the instrumental analysis. Journal of International Environmental Application and Science, 11(2), p.223-228.
15. Ghasemi, A., & Zahediasl, S. [2012]: Normality tests for statistical analysis: a guide for non-statisticians. International journal of endocrinology and metabolism, 10(2), p.486.
16. AS Covariates, B. M. I. [2018]: Multivariate analysis of variance (MANOVA). Multivariate Statistics Made Simple: A Practical Approach, p.73.
17. Trafimow, D. [2019]: A frequentist alternative to significance testing, p-values, and confidence intervals. Econometrics, 7(2), p.26.
18. Wu, L., Li, L., Chen, S., Wang, L., & Lin, X. [2020]: Deep eutectic solvent-based ultrasonic-assisted extraction of phenolic compounds from Moringa oleifera L. leaves: Optimization, comparison and antioxidant activity. Separation and Purification Technology, 247, p.117014.
19. Zeng, J., Ji, M., Zhao, Y., Helmer Pedersen, T., & Wang, H. [2021]: Optimization of electrocoagulation process parameters for enhancing phosphate removal in a biofilm-electrocoagulation system. Water Science and Technology, 83(10), p.2560-2574.
20. Poldrack, R. A., Huckins, G., & Varoquaux, G. [2020]: Establishment of best practices for evidence for prediction: a review. JAMA psychiatry, 77(5), p.534-540.
21. Mohammed A-HA-K, K.Hussain H. [2001]: Deasphaltening and Hydrodesulfurization of Basrah Vacuum Residue. Iraqi J Chem Pet Eng.2: p.12–18.
22. Painter, P.; Veytsman, B.; Youtcheff, J. [2015]: Guide to Asphaltene Solubility. Energy Fuels, 29 (5), p.2951−2961.
23. Morantes, L. R., Percebom, A. M., & Mejía-Ospino, E. [2019]: On the molecular basis of aggregation and stability of Colombian asphaltenes and their subfractions. Fuel, 241, p.542-549.
24. G. Brons and J. M. Yu. [1995]: Solvent deasphalting effects on whole cold lake bitumen. Energy & Fuels, vol. 9, no. 4, p. 641–647.
25. E. Buenrostro-Gonzalez, C. Lira-Galeana, A. Gil-Villegas, and J. Wu. [2004]: Asphaltene precipitation in crude oils: theory and experiments,” AIChE Journal, vol. 50, no. 10, p. 2552–2570.

26. D. Hartmann, H. E. Lopes, C. L. S. Teixeira et al. [2016]: Alkanes induced asphaltene precipitation studies at high pressure and temperature in the presence of argon," Energy & Fuels, vol. 30, no. 5, p. 3693–3706.
27. S. L. Kokal, J. Najman, S. G. Sayegh, and A. E. George. [1992]: Measurement and correlation of asphaltene precipitation from heavy oils by gas injection," Journal of Canadian Petroleum Technology, vol. 31, no. 4, p. 24.
28. S. H. Ng. [1997]: Nonconventional residuum upgrading by solvent deasphalting and fluid catalytic cracking," Energy and Fuels, vol. 11, no. 6, p. 1127–1136.
29. P. Luo, X. Wang, and Y. Gu. [2010]: Characterization of asphaltenes precipitated with three light alkanes under different experimental conditions," Fluid Phase Equilibria, vol. 291, no. 2, p. 103– 110.
30. Shakir, F., Hussein, H., & Abdulwahhab, Z. [2022]: Upgrading of Sharqy Baghdad Heavy Oil via N-Hexane Solvent. Iraqi Journal of Chemical and Petroleum Engineering, 23(3), p.59-66.
31. Hussain, H. K., Ali, S. M., & Ali, Y. M. [2011]: Upgrading Sharky Baghdad Heavy Crude Oil. Al-Khwarizmi Engineering Journal, 7(3), p.19-29.
32. Radhi, A. J. [2012]: Upgrading of East Baghdad Residue by N-Hexane. Doctoral dissertation, University of Technology.
33. Guzmán, J. D., Franco, C. A., & Cortés, F. B. [2017]: An enhanced-solvent deasphalting process: effect of inclusion of SiO2 nanoparticles in the quality of deasphalted oil. Journal of Nanomaterials.
34. Puron, H., Arcelus-Arrillaga, P., Chin, K. K., Pinilla, J. L., Fidalgo, B., & Millan, M. [2014]: Kinetic analysis of vacuum residue hydrocracking in early reaction stages. Fuel, 117: p. 408-414.
35. Keshavarz, B., Houze, E. C., Moore, J. R., Koerner, M. R., & McKinley, G. H. [2020]: Rotary atomization of Newtonian and viscoelastic liquids. Physical Review Fluids, 5(3), p. 33601.
36. Shakir, F., Hussein, H. Q., & Abdulwahhab, Z. T. [2022]: Influence of Nanosilica on Solvent Deasphalting for Upgrading Iraqi Heavy Crude Oil. Baghdad Science Journal, p. 144.
37. Turuga ASS. [2017]: Effect of Solvent Deasphalting Process on the Properties of Deasphalted Oil and sphaltenes From Bitumen. University of Alberta.
38. Adelodun, B., Ajibade, F. O., Ogunshina, M. S., & Choi, K. [2019]: Dosage and settling time course optimization of Moringa oleifera in municipal wastewater treatment using response surface methodology. Desalin. Water Treat, 167, p. 45-56.
39. Palogos, I., Galetakis, M., Roumpos, C., & Pavloudakis, F. [2017]: Selection of optimal land uses for the reclamation of surface mines by using evolutionary algorithms. International Journal of Mining Science and Technology, 27(3), p.491-498.